

# Energetics of Breaking Waves Within the Surf Zone

EDWARD B. THORNTON

*Department of Oceanography, Naval Postgraduate School, Monterey, California 93940*

Surface elevations and velocities were measured for a variety of breaking wave conditions including collapsing, plunging, and spilling breakers. Turbulent and wave-induced velocity components are separated by associating the wave-induced velocities with contribution coherent with the surface. Most of the measurements were made in the lower half of the water column and are indicative of conditions in this region. The average velocity intensity for all experiments was 85% wave induced, indicating that the kinetic energy is primarily wave induced. Remarkably little difference was found between collapsing, plunging, and spilling breakers in terms of percent wave-induced velocity intensity. Breaking waves can be characterized as highly nonlinear with strong wave-wave interactions resulting in energy being transferred away from the primary wave frequency, resulting in a saturation region at higher frequencies. Similarity arguments assuming kinematic instability with phase speed the only relevant parameter suggest a  $-3$  slope for the log-log frequency spectrum of both the surface and horizontal velocities in shallow water. The surface elevation spectra of collapsing and plunging breakers have a slope more closely approximated by a  $-3/2$  slope, indicating the possible importance of surface tension in the breaking processes; the velocity spectra show a  $-3$  slope. The saturation region for spilling breakers surface elevation spectra varied from  $-3$  at lower frequencies to  $-5$  at highest frequencies.

## INTRODUCTION

A primary deficiency in the understanding of sand transport within the surf zone is an adequate knowledge of the kinematics of the water particle motion under breaking waves. Littoral sand transport is a function of the wave and turbulent energies within the surf zone and the longshore current. Turbulence is derived from the wave energy in the dissipation process as the waves propagate across the surf zone. The turbulence and waves act as stirring agents which lift and suspend the sediments. The longshore current is primarily driven by the momentum flux of the coherent wave energy and acts as a net transporting agent for the sand along the shore.

The generation of turbulence under breaking waves occurs at both the surface and bottom boundary layers, as shown schematically in Figure 1. At the surface there is an injection of turbulence due to the breaking wave; the depth of penetration of the turbulence varies with breaker type. Miller [1976] observed the internal velocity field under breaking waves in the laboratory by illuminating bubbles entrained and mixed downward with a collimated light source. Breaking was observed to be initiated by steepening of the free surface at the crest. The crest speed then exceeded the wave velocity, resulting in the crest pitching forward and forming a jet. A vortex is formed as the jet closes with the surface and penetrates into the body of the flow. As the vortex progresses forward and downward, bubbles are entrained and turbulence is generated. Miller found the processes occurring during plunging and spilling breakers to be similar, varying only in the strength and number of vortices generated. The strength of the initial jet determines the qualitative description of plunging or spilling breaker.

Plunging breakers are characterized by a strong jet which generates a vortex that may penetrate to the bottom. The size of the vortex is of the order of the water depth. When the jet strikes the surface, the resulting splash can form second and successive vortices of decreasing strength.

The same processes occur with spilling breakers except that the jet at the crest is weak, giving the appearance of the crest sliding down the face of the wave. The vortex generated is

small, resulting in the turbulence and entrained bubbles being confined to the region above the trough. Hence very little turbulence is injected into the body of the flow under spilling breakers.

Vorticity, or boundary layer momentum, is also diffused upward owing to the bottom shear stress. The height of the boundary layer above the bottom is dependent on bottom roughness, strength of flow, and the time or distance over which the boundary layer has to grow. The velocities near the bed under wave motion oscillate through maxima and zero twice every period. The resulting boundary layer must also pass through two maxima and two zeroes during each period. Hence the bottom boundary layer under waves never has the opportunity to become fully developed and is generally weak, being confined to a region very near the bed.

Outside the surf zone the bottom boundary layer caused by wave action appears to be weak. The primary turbulence mechanisms are the two-dimensional ripple formations characteristic of sandy beds. The ripples act as perturbations to the oscillatory flow near the bed, causing a vortex to be generated near the crest of each ripple; this vortex is diffused upward into the body of the flow field [Tunstall and Inman, 1975].

At the breaker line and inside the surf zone the strength of the flow is intensified and the ripples are planed off, resulting in a flat bed. The bottom is essentially smooth inside the surf zone, and vortex generation by ripples near the bed is not present. Although the strength of the flow is increased inside the surf zone, the bed is plane and the bottom boundary layer remains relatively weak. Therefore the turbulence within the surf zone near the bed and in the water column just above is expected to be small, and the motion should be dominated by the waves.

Breaking of waves can be characterized as a strongly nonlinear process resulting in a transfer of energy away from the primary incident wave frequencies. Energy is transferred to low frequencies, and the process appears to be dominated by resonant excitation of long-edge waves [Sonu *et al.*, 1974; Guza and Bowen, 1976]. The transfer of energy to low frequencies and attendant energy loss through breaking can result in a possible saturation of the run-up spectra [Huntley *et al.*, 1977].

Energy is transferred to high frequencies by strong wave-wave (but not resonant) interactions. The energy transfer is

This paper is not subject to U.S. copyright. Published in 1979 by the American Geophysical Union.

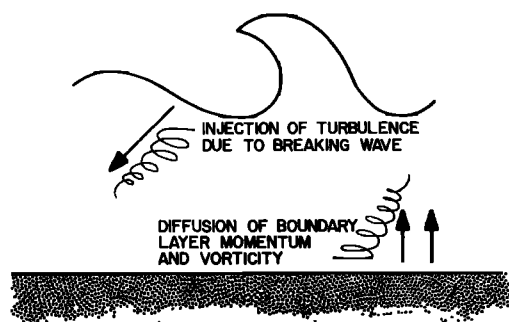


Fig. 1. Generation of turbulence under breaking waves.

evident by the appearance of secondary wave formation [Gallagher, 1972] and corresponding strong harmonic content in the wave spectra [Thornton *et al.*, 1977]. A saturation region in the spectrum of breaking waves would be expected owing to energy transfer to high frequency. Ijima *et al.* [1970], using physical arguments, suggest a saturation region having a  $-1$  slope in the wave spectrum. Huntley and Bowen [1973] suggest an exponential decay of potential energy at high frequency. The redistribution of energy within the frequency spectrum will influence the kinematics of the wave system.

In this paper, velocities and surface elevations are measured in the field for a wide variety of breaking wave conditions. A method for separating the turbulence and wave-induced velocities under waves is used to investigate average turbulent intensities within the surf zone. The manner in which potential and kinetic energies are distributed within the frequency spectra is investigated. The energy spectra are examined with regard to saturation conditions at high frequencies. Similarity arguments are used to explain the form of the saturation region of shallow water waves, and comparisons with measurements are made.

#### EXPERIMENTS

The experiments were designed to measure the kinematics of various types of breaking waves including spilling, plunging, and collapsing breakers. The manner in which waves break depends on the character of the offshore waves and nearshore bottom slope. Waves were measured at three California beaches in order to include the three breaker types.

Plunging and spilling breakers were measured at Del Monte Beach, which is located in the extreme southern part of Monterey Bay. The median grain size at Del Monte Beach is approximately 0.2 mm (taken at the mean water line), and the beach slope varies from 1:14 to 1:40. The waves at this location are generally topographically sheltered, and severely directionally filtered owing to refraction by the geometry of the bay, usually resulting in swell-type waves impinging perpendicular to the shore. Hence a simplification to a two-dimensional narrow banded wave description is allowed.

Collapsing and plunging breakers were measured at Carmel River Beach, Carmel, at which the median sand size is approximately 0.6 mm, and the beach slope varies from 1:6 to 1:12. Carmel River Beach is also within an embayment, where the generally narrow band waves impinge almost perpendicular to shore.

Spilling breakers were measured at Torrey Pines Beach at La Jolla; this site was selected because of the relatively uncomplicated offshore bathymetry with generally straight and parallel bottom contours. The median sand grain size is approximately 0.1 mm, and the beach slope varies from 1:40 to 1:150. The coastline here is sheltered by offshore islands such

that waves derived from deep water can only come from selected directions because of island sheltering. Locally derived sea waves were often superposed on the swell during the measurement period, resulting in a two-dimensional broad band spectrum.

Capitance wave gauges and two-component current meters were used to measure surface elevations and velocities in a vertical plane beneath the surface measurements. The current meters were Marsh-McBirney Model 721 and 722 electromagnetic flow meters. The instruments were mounted on towers, each 4 m in height. The towers were made of a 2-inch pipe and were guyed and anchored at four points. Typically, three towers were placed on a line perpendicular to the shore and were erected during low tide, when the beach was easily accessible. The measurements were then conducted at high tide. The tidal range was typically 2 m. The details of the instrumentation and their construction and calibration and the details of installation of equipment and difficulties encountered (there were many) are described by Thornton *et al.* [1977].

#### SEPARATING WAVE-INDUCED AND TURBULENT VELOCITY COMPONENTS

Spectra and cross spectra between surface elevations and onshore-offshore horizontal velocities were calculated for all experiments. Correlation functions were calculated using a maximum lag of 5% of the record length. A Parzen window was applied to the correlation functions. Spectra were computed by Fourier transforming the correlation functions. The resulting power spectral estimates contain  $74^\circ$  of freedom.

An example of spectra measured for spilling breakers at Torrey Pines Beach is shown in Figure 2. The waves were breaking either at or shoreward of the measurement location during this particular experiment. The surface elevation and velocity spectra are very similar in form except at the lowest frequencies. Definite harmonics of the primary wave frequency at 0.07 Hz (14 s) are evident, whereas the incident wave field measured offshore was relatively broader and showed no harmonics.

The coherence spectrum is typical of all the breaking waves measured, showing high coherence over the band of predominant wave energy. The percent coherence at the peak of

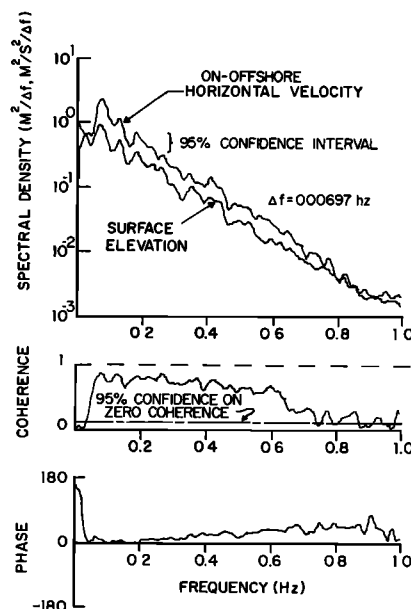


Fig. 2. Surface elevation and horizontal velocity spectra for spilling breakers Torrey Pines Beach, March 21, 1977.

the spectrum is 0.83. The 95% significance level for zero coherence is indicated. The coherence value corresponding to the peak energy in the spectra for all experiments ranged above 0.78 (see Table 1). The measured phase difference between the surface and horizontal velocity shown at the bottom of Figure 2 is small at the peak of the spectrum, which is in accord with wave theory. The slight increase in phase difference toward higher frequency is attributed to electronic filtering by the flow meter.

Examples of spectra calculated for plunging breakers on Del Monte Beach and collapsing breakers on Carmel River Beach are given by Thornton *et al.* [1977]. The spectra of plunging and collapsing breakers are very similar to those shown in Figure 2 for spilling breakers except that the harmonics are generally more pronounced owing to the waves being more narrow banded and more strongly nonlinear. The high coherence between surface elevation and horizontal velocity beneath and the similarity of the spectra indicates that most of the energy is associated with the surface or is wave induced.

A simple technique to separate the measured turbulent and wave-induced velocity components follows. The wave-induced velocity contribution is defined as that portion of the velocity field which is coherent with the wave surface elevation. By definition, all motion of the surface is wave motion. The incoherent portion of the velocity field is assumed to be turbulent.

The velocity can be separated into contributions of a mean plus wave-induced and turbulent components:

$$u_i = \bar{u}_i + \tilde{u}_i + u'_i, \quad i = 1, 2, 3 \quad (1)$$

For convenience it will be assumed that the mean value  $\bar{u}_i$  is

subtracted out of the signal or is zero. The following analysis relates only to the horizontal velocity component normal to the beach, although the analysis is applicable to all components; hence the indices are dropped. The spectrum of the horizontal velocity can be expressed in terms of the wave-induced and turbulent contributions

$$S_u(\omega) = S_{\tilde{u}}(\omega) + S_{u'}(\omega) + S_{\tilde{u}u'}(\omega) + S_{u'\tilde{u}}(\omega) \quad (2)$$

where  $\omega$  is radial frequency.

Conceptually, there are several sources of turbulence within the surf zone. 'Background' turbulence can be advected into the surf zone from sources outside the region and would be expected to be statistically independent of the waves. Mechanisms for generating turbulence by the waves within the surf zone result in various time scales of motion. Any turbulence generated by the straining of the fluid particles by the wave motion would be at scales much smaller than the wave scales and hence separated in frequency. Turbulence generated at the bed is diffused or advected upward on both the forward and backward motion of the wave such that turbulence would appear at twice the frequency of the waves. The primary generation of turbulence occurs at breaking. Turbulence is generated every time a wave breaks by the injection of the plunging crest into the fluid column. The size of the vortices, at least under plunging and collapsing breakers, is of the same scale as the orbital motion induced by the wave. The vortices would then break down into smaller scales of turbulence. Hence there can be some correlation between turbulence and wave-induced motion.

As a first approximation, it will be assumed the wave-induced and turbulent velocity spectral components (at a partic-

TABLE 1. Data Summary at Measurement Locations

Run	Distance Across Surf Zone, %	Beach Slope, tan $\beta$	Mean Water Depth $h$ , cm	Relative Flow Meter Elevation from Bottom, $z/h$	Frequency of Peak Coherence $f_0, h_z$	Peak Coherence $\gamma_{u\eta}^2(f_0)$	Surf Elevation Variance $\sigma_\eta^2, m^2$	Velocity Variance $m^2/s^2$	Surface Parameter $\xi$	Wave-Induced Velocity Intensity $\sigma_{\tilde{u}}/\sigma_u, \%$
Carmel River										
May 29, 1975	0*	0.14	145	0.33	0.079	0.78	0.036	1.12	0.25	0.84
May 10, 1976	0.3†	0.12	46	0.33	0.087	0.82	0.008	1.78	0.19	0.81
Del Monte										
April 12, 1973	0	0.03	186	0.26	0.067	0.79	0.025	0.22	4.7	0.82
May 23, 1974	-0.1‡	0.03	148	0.36	0.125	0.94	0.029	0.17	6.9	0.84
March 4, 1975	0	0.07	125	0.46	0.061	0.94	0.048	0.93	0.67	0.85
March 4, 1975	0.1	0.07	45	0.24	0.067	0.94	0.026	0.69	0.49	0.80
March 5, 1975	-0.1	0.06	167	0.35	0.078	0.87	0.017	0.27	0.69	0.80
March 5, 1975	0	0.06	108	0.31	0.084	0.93	0.023	0.32	0.82	0.81
March 6, 1975	-0.1	0.04	130	0.28	0.084	0.95	0.015	0.15	2.0	0.82
March 8, 1975	0	0.04	115	0.49	0.092	0.94	0.015	0.18	2.0	0.90
March 8, 1975	0.1	0.04	62	0.66	0.092	0.92	0.018	0.35	2.2	0.76
March 9, 1975	0.4	0.03	102	0.39	0.061	0.84	0.020	0.28	4.4	0.70
March 9, 1975	0.5	0.03	67	0.70	0.061	0.83	0.013	0.36	3.6	0.64
Torrey Pines										
March 16, 1977	0.3	0.007	136	0.35	0.070	0.90	0.045	0.16	85	0.90
March 17, 1977	0.3	0.009	176	0.28	0.077	0.85	0.059	0.15	74	0.88
March 18, 1977	0.1	0.009	180	0.25	0.084	0.84	0.043	0.26	75	0.81
March 21, 1977	0.1	0.010	153	0.33	0.070	0.83	0.036	0.16	39	0.87
March 21, 1977	0.5	0.009	96	0.15	0.070	0.79	0.017	0.08	30	0.87
March 23, 1977	0.1	0.016	151	0.44	0.070	0.91	0.041	0.18	16	0.91
March 23, 1977	0.5	0.016	62	0.35	0.070	0.86	0.008	0.07	6.9	0.90

0 = break point.

\*Average breaker location.

†Positive number indicates shoreward of breakpoint.

‡Negative number indicates outside surf zone.

ular frequency  $\omega$ ) are statistically independent. The cross spectra between wave-induced and turbulent velocities on the right side of (2) are then zero, and the horizontal velocity spectrum simplifies to

$$S_u(\omega) = S_{\bar{u}}(\omega) + S_{u'}(\omega) \tag{3}$$

The problem can be solved by allowing the turbulent velocities to be correlated with the waves, but this method does require knowing the spectral transfer function between surface elevation and velocity field. A spectral transfer function derived from linear wave theory has been used by *Thornton et al.* [1977] to calculate velocities beneath breaking waves; a comparison of the measured and calculated velocities showed that this technique was limited to mild breaking conditions and was not generally applicable. Therefore the assumption of statistical independence is made, which greatly simplifies the analysis, and the results are examined as to the importance of this assumption.

Initially, it is assumed the waves are long crested and unidirectional and approach perpendicular to the beach so that the crests are aligned normal to the horizontal velocity components. Using the assumption of statistical independence between wave-induced and turbulent velocities, the cross spectrum between surface elevation and horizontal velocity is given by

$$S_{u\eta}(\omega) = S_{\bar{u}\eta}(\omega) \tag{4}$$

where the contribution to the cross spectrum by turbulence is zero.

It is further assumed that the waves and wave-induced velocities are described by a constant parameter linear process where the coherence is identically equal to unity

$$\gamma_{\bar{u}\eta}^2(\omega) = \frac{|S_{\bar{u}\eta}(\omega)|^2}{S_{\bar{u}}(\omega)S_{\eta}(\omega)} \equiv 1 \tag{5}$$

The substitution of (3), (4), and (5) into the definition of coherence between the total horizontal velocity and surface elevation results in

$$\gamma_{u\eta}^2(\omega) = \left[ 1 + \frac{S_{u'}(\omega)}{S_{\bar{u}}(\omega)} \right]^{-1} = \frac{S_{\bar{u}}(\omega)}{S_u(\omega)} \tag{6}$$

Increasing lack of coherence is due to an increasingly high ratio of turbulence (noise) to coherent wave-induced velocity fluctuations (signal). The coherence indicates the percent of the velocity spectrum that is associated with the wave surface.

The wave-induced velocity can be calculated using (6):

$$S_{\bar{u}}(\omega) = \gamma_{u\eta}^2(\omega)S_u(\omega) \tag{7}$$

The percent of wave-induced velocity intensity (ratio of wave-induced to total velocity intensities) calculated using the coherence function (equation (6)), is shown in Figure 3. The velocity intensity was calculated as the square root of the variance. The variance was obtained by integrating the velocity spectrum across the sea swell band from 0.03 Hz (30-s period) to the nyquist frequency of 2.5 Hz,

$$\sigma_u = \left[ \frac{1}{2\pi} \int_{\omega_1}^{\omega_n} S_u(\omega) d\omega \right]^{1/2} \tag{8}$$

The variance of the wave-induced velocity was calculated in the same manner, using the wave-induced velocity spectrum expressed by (7). Considerable energy density or variance contribution was present at low frequencies in a number of experiments owing to variability in the mean currents or low-frequency

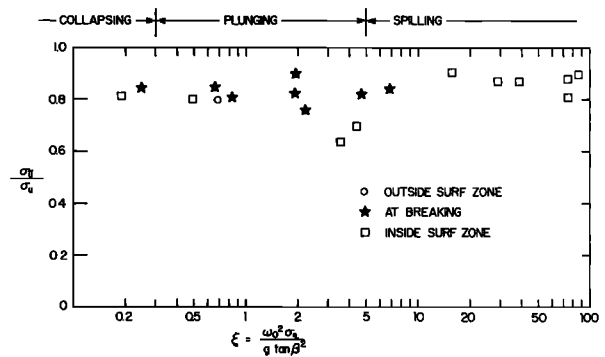


Fig. 3. Percent wave-induced velocity intensity under breaking waves.

quency edge waves or surf beat. This low-frequency energy was effectively filtered out in the variance calculation by placing a lower limit of 0.03 Hz on the integration.

The percent wave-induced velocity intensity is plotted against the local breaking wave parameter

$$\xi = \frac{\omega_0^2 \sigma_\eta}{g \tan^2 \beta} \tag{9}$$

where  $\omega_0$  is the radial frequency at the peak of the wave spectrum,  $\sigma_\eta$  is the local rms wave height, and  $\tan\beta$  is the beach slope. *Battjes* [1975] showed that the breaking wave type could be classified using this parameterization, and the breaker type has been denoted for various values of  $\xi$  in Figure 3. It is emphasized the breaking wave parameter refers to local wave conditions in comparison with conditions at breaking, as was used by *Battjes* [1975]. Even with this limitation, the observed breaking wave type agreed very well with the breaker classification. The stars denote waves measured at breaking.

A difficulty in the interpretation of point measurements of breaking waves is that the breaker locations wander, resulting in a wave field that is not spatially homogeneous. To a first approximation the height of a breaking wave is proportional to the local mean water depth. Therefore breaker location will vary, depending on the incident wave height and changes in the mean water level. Changes in the mean water level can occur owing to long waves such as surf beat with periods of the order of minutes or owing to tidal variations with periods of 12 or 24 hours.

The locations of the measurements within the surf zone are given in column 2 of Table 1 as the percent distance shoreward of the average breaker location in relation to the width of the surf zone. The surf zone is compressed on steep beaches and stretched on shallow sloping beaches. On the steep Carmel River Beach the point of wave breaking was relatively constant, and the measurements were made at or just inside the breaker point. The Del Monte Beach had a wider surf zone, and measurements were made outside, at, and inside the surf zone, as noted. The surf zone was very wide on the shallow sloping beach at Torrey Pines, and all measurements were essentially inside the surf zone. The breaker location is denoted in Figure 3; stars indicate waves measured at breaking, squares denote waves measured inside the surf zone, and circles denote waves just outside the surf zone.

The measurements show a surprisingly small spread of values for the ratio of wave-induced to total velocity intensity over a wide variety of breaker conditions, ranging from collapsing to spilling breakers, with the local breaking waves parameter  $\xi$  varying over 3 decades. There appears to be little

difference between conditions measured at breaking or inside the surf zone.

The results show that on the average, more than 85% of the velocity intensity is wave induced. Stated in terms of the average kinetic energy, more than 70% is associated with the waves and less than 30% is due to turbulence.

Turbulence is primarily generated at the surface during breaking and is advected and diffused downward. A second but weaker turbulent boundary layer is formed at the bottom, with turbulent momentum transferred upward. Therefore the percent of turbulent energy would be expected to be dependent on the elevation of measurement. The measurements for all runs are summarized in Table 1. The distance of the flow meter above the bottom in relation to the average depth of water is given in column 5 and shows that most of the measurements were made in the lower third of the water column. Only two measurements were made above mid-depth, and these measurements represent two of the lowest values of the percent wave-induced velocity intensity (highest turbulence) measured. Hence the depth of measurement can obviously be important. The measurements here pertain to the conditions nearer the bed, which is the region of interest for sediment transport studies.

The wave-induced velocity contribution to the total velocity varies with frequency. The percent wave-induced kinetic energy is measured as a function of frequency by the coherence, which was a maximum (or very close to a maximum) at the point of peak energy density of the spectrum. The coherence corresponding to the peak in the spectrum is given in column 7 of Table 1. The coherence maxima average 0.90 for Carmel River and Del Monte Beaches, where the waves were long crested and impinged perpendicular to the beach. The average value of coherence maxima for Torrey Pines Beach is slightly less at 0.85 for spilling breakers; the decreased value is interpreted as at least partially being caused by the short crestedness of the incident wave field.

Coherence is decreased owing to waves approaching at an angle to the flow meter alignment or because the waves are short crested. During the Torrey Pines Beach experiments, relatively short crested waves approaching at small angles of 0°-15° between crest and bottom contour often occurred. The decrease in coherence due to short crestedness and directionality results in a slight underestimate of the wave-induced velocities.

Yefimov and Khristoforov [1971] examined the effects of wave directionality and short crestedness on coherence between waves and horizontal velocity. They described long-crested waves using a train of two-dimensional, planar random waves traveling in direction  $\theta_0$ ,

$$\psi_{\eta}(\omega, \theta_1) = S_{\eta}(\omega)\delta(\theta - \theta_0) \tag{10}$$

where  $\delta(\theta - \theta_0)$  is the Dirac delta function. The percent decrease of coherence due to long crested waves approaching at an angle  $\theta_0$  in comparison with the case of long-crested ( $lc$ ) normal incidence is given by

$$\frac{\gamma_{u\eta}^2(\omega, \theta_0)|_{lc}}{\gamma_{u\eta}^2(\omega)} = \left[ \frac{1}{\cos^2 \theta_0} + \frac{S_{\bar{u}}(\omega)}{S_u(\omega)} \left( 1 - \frac{1}{\cos^2 \theta_0} \right) \right]^{-1} \tag{11}$$

Short-crested waves are described as a train of three-dimensional waves whose directional spreading is assumed to be of the form

$$\psi_{\eta}(\omega, \theta_s) = (2/\pi)S_{\eta}(\omega) \cos^2(\theta - \theta_0), 0 \quad \text{for } |\theta - \theta_0| > \pi/2 \tag{12}$$

For the case of short-crested waves ( $sc$ ) approaching at an angle in comparison with long-crested normal incidence,

$$\frac{\gamma_{u\eta}^2(\omega, \theta_0)|_{sc}}{\gamma_{u\eta}^2(\omega)} = \left[ \frac{4}{3} + \frac{1}{3} \frac{S_{\bar{u}}(\omega)}{S_u(\omega)} (\tan^2 \theta_0 - 1) \right]^{-1} \tag{13}$$

Table 2 gives the ratio of coherence decrease due to wave directionality and short crestedness for a ratio of  $S_{\bar{u}}(\omega)/S_u(\omega) = 0.8$ . The results show that the coherence is decreased very little owing to long-crested waves approaching at an angle. Short-crested waves decrease the coherence by a maximum of less than 10% for the wave directions encountered during the experiments. It is noted that even at zero mean angle of incidence the coherence is reduced owing to the effect of short crestedness as the result of wave energy spread over many directions. If a correction factor is applied to the Torrey Pines data for the effects of short crestedness, the percent of wave-induced velocity for spilling breakers is increased.

Deficiencies of the proposed model are due to the assumed statistical independence between waves and turbulence and to nonlinearities inherent to breaking wave processes. Further, it has been tacitly assumed that instrumentation noise is negligible. The coherence between surface elevation and velocity will be increased if turbulence and waves are correlated, i.e., statistically dependent; an analysis performed showed the maximum error to be of the order of a 10% overestimation of the wave-induced kinetic energy. On the other hand, the linear coherence between waves and velocities will always be decreased owing to nonlinearities which are strong in a breaking wave and to directional spreading of the incident wave energy, resulting in an underestimation of the wave-induced kinetic energy. Instrumentation noise (although negligibly small for the measurement system used) would also decrease coherence between surface elevation and velocity, acting in the same manner in (6) as the turbulence.

In summary, the deficiencies in the model appear to result in small errors, which tend to balance. The errors are greatest under plunging breakers, where the waves and turbulences would have highest correlation, but at the same time the nonlinearities are strongest. The errors would be small under spilling breakers. Because of high coherence (generally above 0.90) between the measured velocities and surface elevation, it is reasoned that the assumption of a constant parameter linear system is a good first approximation, which implies linearity and statistical independence. Hence the estimates of the percent of wave-induced kinetic energy are considered reasonable and probably conservative (underestimates).

The separation of wave-induced and turbulent velocities using the spectral technique suggested is an averaging process. The percent wave-induced velocity is averaged over the wave period and over many waves. In the course of the passage of a single breaking wave, turbulence is injected as bursts into the water column. Caution should be applied in translating the results to the sediment transport problem, for it may be the

TABLE 2. Ratio of Coherence Decrease Due to Wave Directionality and Short Crestedness,  $S_{\bar{u}}(\omega)/S_u(\omega) = 0.8$

$\theta_0$ , deg.	$\frac{\gamma_{u\eta}^2(\omega, \theta_0) _{\text{long crest}}}{\gamma_{u\eta}^2(\omega)}$	$\frac{\gamma_{u\eta}^2(\omega, \theta_0) _{\text{short crest}}}{\gamma_{u\eta}^2(\omega)}$
0	1.00	0.94
10	0.99	0.93
20	0.97	0.91
30	0.94	0.87

few bursts of turbulence that dominate the process, while the majority of the time the water column is dominated by coherent wave motion.

#### SATURATION REGION IN THE SPECTRUM OF BREAKING WAVES

Wave breaking occurs due to kinematic instability when fluid particles at the crest of the free surface are moving forward with a speed greater than the wave speed  $C$ ; this has been verified in the laboratory both for waves in deep water that are 'white capping' [Banner and Phillips, 1974] and for shoaling waves breaking on a beach [Miller, 1976]. Waves approaching breaking are highly nonlinear with strong wave-wave interactions resulting in energy being transferred from low frequencies to higher frequencies. The energy is transferred down the spectrum and is eventually dissipated by viscosity at the highest frequencies. Breaking occurs when the transfer of energy is not fast enough to balance the increase in energy density of the waves during shoaling; i.e., the waves are 'saturated' with energy. A saturation region would be expected through which energy is transferred from the low to high frequencies. The excess energy is dissipated in the form of turbulence and air entrainment as the crest of the wave spills or plunges over the wave face.

The rate of shoaling determines the rate at which excess energy must be dissipated. Shoaling is governed by the beach steepness, depth of water, and height of the wave. Spilling breakers most commonly occur on gently sloping beaches, since spilling breakers shoal slowly. The energy is slowly dissipated in the crest of the wave. Plunging breakers result when waves rapidly shoal over a generally steeper beach, resulting in violent plunging and rapid dissipation of energy.

Using similarity arguments and assuming breaking occurs as a result of kinematic instability for which the only governing parameters is the wave speed, Thornton [1977] showed that in deeper water outside the surf zone the saturation region of the wave spectrum below the frequencies at which surface tension  $\xi$  and viscosity  $\nu$  are important is given by

$$S_{\eta}(\omega) \sim C^2 \omega^{-5} \quad \omega < \omega_{\xi} < \omega_{\nu} \quad (14)$$

In deep water,  $C = g\omega^{-1}$ , so

$$S_{\eta}(\omega) = B_d g^2 \omega^{-5} \quad (15)$$

where  $B_d$  is an assumed constant. Equation (15) is in agreement with Phillips' [1958a] earlier derivation, which assumed a dynamic instability criterion. In shallow water the waves become nondispersive, and the wave speed is a function of the depth  $h$ , but

$$C = (gh)^{1/2} \quad (16)$$

so the saturation region of the spectrum is given by

$$S_{\eta}(\omega) = B_s gh \omega^{-3} \quad (17)$$

where  $B_s$  is a constant presumably different from the deep water constant  $B_d$ . The results state that energy is slowly transferred down the spectrum in deep water, as evidenced by the steep  $-5$  slope, presumably by weak nonlinear interactions. As waves propagate into shallow water, shoaling occurs and waves steepen. Energy is more rapidly transferred to higher frequencies, as evidenced by the less steep  $-3$  slope in the saturation range of the spectrum.

The horizontal velocity spectrum can be calculated in the saturation region from the surface elevation spectrum by ap-

plying the spectral transfer function  $H_{\bar{u}}(\omega)$ , derived from linear theory,

$$S_{\bar{u}}(\omega) = |H_{\bar{u}}(\omega)|^2 S_{\eta}(\omega) \quad (18)$$

where

$$H_{\bar{u}}(\omega) = \frac{\omega \cosh k(h+z)}{\sinh kh} \quad (19)$$

For deep water,

$$S_{\bar{u}}(\omega) = B_d g^2 \omega^{-5} \quad (20)$$

and for shallow water,

$$S_{\bar{u}}(\omega) = B_s g^2 \omega^{-3} \quad (21)$$

It is noted that the velocity saturation region is the same for both deep and shallow water.

The  $-5$  slope in the saturation region of the deep water wave spectrum has been verified by a number of investigators [see Phillips, 1966]. Experimental evidence suggesting the validity of the saturation regions of the deep water velocity spectrum (equation (20) is given by Thornton [1977], and the shallow water wave and velocity spectra, equations (17) and (21), are given by Kitaigorodskii *et al.* [1975] and Thornton [1977]).

The importance of surface tension in breaking wave processes was noted by Miller [1973]. At breaking, the waves become very steep, with sharp crests. The curvature in the neighborhood of the crest, particularly for plunging breakers, becomes very large, so surface tension forces become locally important. Phillips [1958b], using dimensional arguments, showed that when surface tension is the only important parameter, the frequency wave spectrum is given by

$$S_{\eta}(\omega) = B_t \xi^{2/3} \omega^{-7/3} \quad \omega_{\xi} < \omega < \omega_{\nu} \quad (22)$$

Spectra of surface elevation for the cases of plunging and collapsing breakers are shown in Figure 4 plotted on a log-log scale. The spectral estimates have been block averaged over frequency bands such that the log energy values are linearly distributed on the log frequency axis. The confidence interval shown on the figure decreases with increasing frequency because of the increasing number of frequency bands over which spectral estimates are averaged. The slope of the spectra at high frequencies more closely approximates a  $-3/2$  slope than a  $-3$  slope, indicating the possible importance of surface tension in breaking processes, as indicated by (22). It is not apparent that surface tension should dominate the spectra over the wide range of frequencies indicated, since the corresponding wavelengths at the lower frequencies far exceed the capillary range. It should be noted that the  $-3/2$  slope dependence in the spectra was observed by the author before realizing a possible physical explanation, as provided by (22).

The onshore horizontal velocity spectra are shown in the bottom of Figure 4. The slopes of the velocity spectra at high frequencies are most closely approximated by a  $-3$  slope. The surface and velocity spectra are not consistent with the saturation spectra derived using similarity arguments. The saturation region of the velocity spectrum would appear associated with a surface on which surface tension is not important, whereas the surface elevation spectra suggests that surface tension dominates the saturation region.

The spectra do suggest that the potential energy of waves at breaking is more rapidly transferred to higher frequencies, as evidenced by the  $-3/2$  slope in the spectra in comparison with

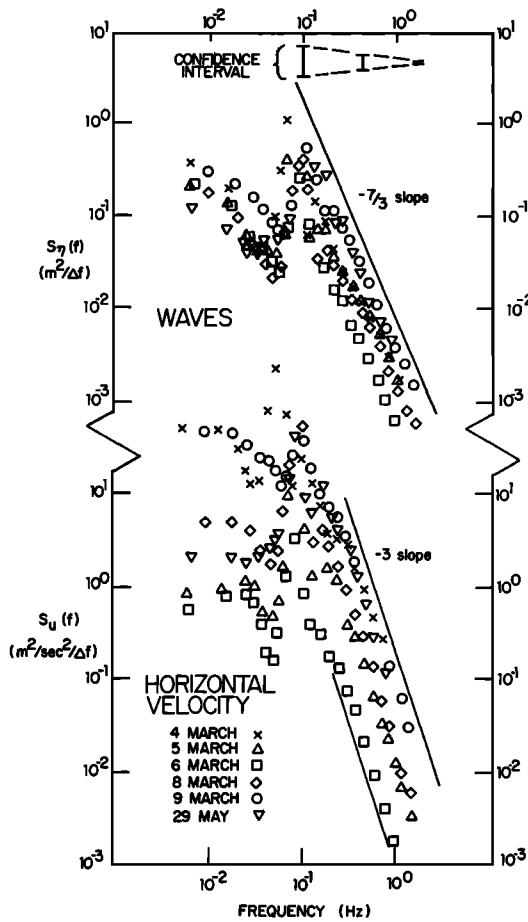


Fig. 4. Surface elevation and horizontal velocity spectra of collapsing and plunging breakers.

the kinetic energy of the waves, as shown by the steeper  $-3$  slope at high frequencies. The difference in the rate of energy transfer contributes to an unequal partitioning of potential and kinetic energies in breaking waves.

On the basis of the similarity arguments presented, the spectra in the saturation region would be expected to overlie each other, provided the coefficients of (15–21) are constant. The energy saturation of breaking waves is similar but opposite to that which occurs during wave generation. During wave generation, saturation starts with the shortest waves, or highest frequencies, and the spectrum ‘fills’ from the highest to lowest frequencies. There is an upper bound on the energy density of the shortest waves, since there is a maximum wave steepness that cannot be exceeded. The excess energy is either dissipated or goes to build the next longer waves and so forth. Therefore the saturation region of waves during generation in deep water has the same energy density that is fixed by the shortest waves, and various spectra overlie each other in the saturation region no matter what the total variance of the waves. For this reason the coefficient  $B_d$  in (15) has been found to be a constant for saturated waves during wave generation [Phillips, 1966].

During shoaling and breaking of waves on a beach the waves first become saturated at the peak energy density, and energy is transferred down the spectrum to form the higher-frequency saturated region. Hence the energy density level of the saturation region would be expected to be a function of the energy density at the primary breaking wave frequency. Since, to a first approximation, breaking wave height has been found

to be proportional to the depth, the local depth imposes a bound on the energy density at the primary frequency and also on the total energy density.

As can be seen in Figure 4, the wave and horizontal velocity spectra do not overlie each other in the saturation region. In order for the high-frequency saturation spectra to collapse to a single line the coefficient  $B_s$  of (21) must assume some functional relationship and cannot be a constant. Considerable effort was expended in seeking such a functional relationship for  $B_s$ , considering the beach slope, depth, wave variance, and primary wave frequency, but with no satisfactory conclusion.

The surface elevation spectra of the spilling breaker conditions at Torrey Pines are shown in Figure 5. Surprisingly, the high-frequency region is more closely approximated by a  $-5$  slope corresponding to saturation conditions in deep water. Surface tension does not appear to dominate the less steep spilling breakers. Spilling breakers are not as strongly non-linear, so the spectral components at higher frequencies might act as free waves and not be phase locked, or coupled, to the low-frequency components. High-frequency wave components acting as free waves can be categorized as deep or intermediate depth waves, according to linear wave theory. For example, in 1 m of water, wave components with frequencies between 0.16 and 0.85 Hz (6.4- to 1.1-s periods) are classified as intermediate depth water waves, and wave components having

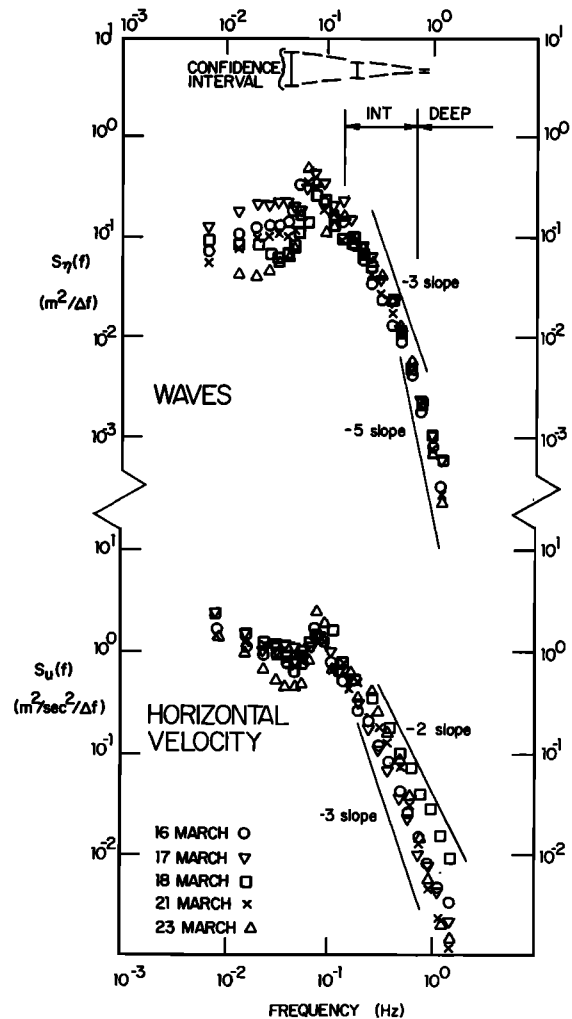


Fig. 5. Surface elevation and horizontal velocity spectra of spilling breakers.

frequencies greater than 0.85 Hz are classified as deep water waves. Hence the slope of the saturation region would be expected to change from  $-3$  at the lower frequencies to  $-5$  at the highest frequencies. The classification of wave components for 1-m depth water is shown in Figure 5.

The velocity spectra for spilling breakers exhibit slopes varying between about  $-\frac{3}{2}$  or  $-2$  to  $-3$  at high frequencies. Isotropic turbulence in the inertial subrange in the frequency spectrum exhibits equilibrium ranges having slopes of  $-\frac{3}{2}$ , corresponding to highly convected flow, and  $-2$ , corresponding to slowly convected flow [Seitz, 1971]. The slope of the spectrum would depend on the strength of the mean flow and the relative intensities of the wave-induced and turbulent velocities in the saturation range. Whereas the mean longshore velocities at Del Monte and Carmel were essentially zero, the average longshore currents during the Torrey Pines experiments ranged from near zero to over 1 m/s. Conditions of fully developed turbulent boundary layer flow could be approximated in the alongshore direction, resulting in near isotropic turbulence.

#### CONCLUSIONS

Surface elevations and velocities were measured for a variety of breaking wave conditions including collapsing, plunging, and spilling breakers. A method for separating turbulence and wave-induced velocity contributions is presented. The results show that most of the kinetic energy is coherent with the surface and therefore wave induced. Most of the measurements were made in the lower half of the water column and are indicative of conditions in this region. The average velocity intensity for all experiments was 85% wave induced. In terms of average kinetic energy, more than 70% is associated with the waves, and less than 30% is due to turbulence. The results showed remarkably little difference between collapsing, plunging, and spilling breakers in terms of percent wave-induced velocity intensity.

Breaking waves can be characterized as highly nonlinear with strong wave-wave interactions resulting in energy being transferred away from the primary wave frequency. Breaking occurs when the transfer of energy to higher frequencies is not fast enough to balance the increase in energy density of the waves during shoaling. At breaking and inside the surf zone the waves can be characterized as energy saturated, and a saturation region in the energy density spectrum results. Similarity arguments, assuming kinematic instability with phase speed the only relevant parameter, suggest a  $-3$  slope for the saturation region of a log-log frequency spectrum of both the surface and horizontal velocities in shallow water.

The surface elevation spectra of collapsing and plunging breakers has a slope more closely approximated by a  $-\frac{3}{2}$  slope, indicating the possible importance of surface tension in the breaking processes. The horizontal velocity spectra closely approximated a  $-3$  slope in the saturation region, which, although agreeing with similarity arguments, is inconsistent with the observed  $-\frac{3}{2}$  slope in the surface spectra.

Spilling breakers are weakly nonlinear such that the wave components can act as free waves propagating dispersively with their own phase velocity. The surface elevation spectra reflect saturation conditions based on dispersive phase speeds such that the slope varied from  $-3$  at lower frequencies, indicative of shallow water wave components, to  $-5$  at highest frequencies, indicative of deep water wave components. For

the case of waves obliquely approaching the beach on which longshore currents are generated, the saturation region of the velocity spectrum can be contaminated by turbulence.

*Acknowledgments.* The data collected at Torrey Pines Beach was measured in cooperation with Robert T. Guza and the Shore Processes Laboratory at Scripps Institution of Oceanography. This work was supported by the Office of Naval Research, Geography Branch, under contract NR 388-114.

#### REFERENCES

- Banner, M. L., and O. M. Phillips, On the incipient breaking of small-scale waves, *J. Fluid Mech.*, **4**, 646-656, 1974.
- Battjes, J., Surf similarity, in *Proceedings of the Fourteenth Conference on Coastal Engineering*, pp. 466-479, American Society of Civil Engineers, New York, 1975.
- Gallagher, B., Some qualitative aspects of nonlinear wave radiation in a surf zone, *Geophys. Fluid Dyn.*, **3**, 347-354, 1972.
- Guza, R. T., and A. J. Bowen, Resonant interactions for wave breaking on a beach, in *Proceedings of the 15th Coastal Engineering Conference*, pp. 560-579, American Society of Civil Engineers, New York, 1976.
- Huntley, D. A., and A. J. Bowen, Comparison of the hydrodynamics of steep and shallow beaches, in *Nearshore Sedimentation*, edited by J. Hails and A. Carr, pp. 69-109, John Wiley, New York, 1975.
- Huntley, D. A., R. T. Guza, and A. J. Bowen, A universal form for shoreline runup spectra? *J. Geophys. Res.*, **82**(18), 2577-2581, 1977.
- Ijima, T., T. Matsuo, and K. Koga, Equilibrium range spectra in shoaling water, in *Proceedings of the Twelfth Conference on Coastal Engineering*, pp. 137-150, American Society of Civil Engineers, New York, 1970.
- Kitaigorodskii, S. A., V. P. Krasitskii, and M. M. Zaslavskii, On Phillips' theory of equilibrium range in the spectra of wind-generated waves, *J. Phys. Oceanogr.*, **5**, 410-420, 1975.
- Miller, R. L., The role of surface tension in breaking waves, in *Proceedings of the Thirteenth Conference on Coastal Engineering*, pp. 433-449, American Society of Civil Engineers, New York, 1973.
- Miller, R. L., Role of vortices in surf zone prediction: Sedimentation and wave forces, Beach and Nearshore Sedimentation, *Spec. Publ. 24*, pp. 92-114, Soc. of Econ. Paleontol. and Mineral., 1976.
- Phillips, O. M., The equilibrium range in the spectrum of wind-generated waves, *J. Fluid Mech.*, **4**, 425-434, 1958a.
- Phillips, O. M., On some properties of the spectrum of wind generated ocean waves, *J. Mar. Res.*, **16**, 231-245, 1958b.
- Phillips, O. M., *The Dynamics of Upper Ocean*, 261 pp., Cambridge University Press, New York, 1966.
- Seitz, R. C., Measurements of a three-dimensional field of water velocities at a depth of one meter in an estuary, *J. Mar. Res.*, **29**, 140-150, 1971.
- Sonu, C. J., N. Pettigrew, and R. G. Fredericks, Measurements of swash profile and orbital motions on the beach, in *Proceedings of the International Symposium on Ocean Wave Measurement and Analysis*, pp. 621-638, American Society of Civil Engineers, New York, 1974.
- Thornton, E. B., Rederivation of the saturation range in the frequency spectrum of wind generated gravity waves, *J. Phys. Oceanogr.*, **7**(1), 137-140, 1977.
- Thornton, E. B., D. P. Richardson, F. L. Bub, and J. J. Galvin, Kinematics of breaking waves in the surf zone, in *Proceedings of the Fifteenth Conference on Coastal Engineering*, pp. 461-476, American Society of Civil Engineers, Ann Arbor, Michigan, 1977.
- Tunstall, E. B., and D. L. Inman, Vortex generation by oscillatory flow over rippled surfaces, *J. Geophys. Res.*, **80**(24), 3475-3484, 1975.
- Yefimov, V. V., and G. N. Khristoforov, Spectra and statistical relations between the velocity fluctuations in the upper layer of the sea and surface waves, *Atmos. Oceanic Phys.*, **7**(12), 1290-1310, 1971.

(Received May 2, 1978;  
revised April 6, 1979;  
accepted April 11, 1979.)